International Journal of Biological Macromolecules 111 (2018) 33–38

Contents lists available at ScienceDirect

International Journal of Biological Macromolecules

journal homepage: http://www.elsevier.com/locate/ijbiomac

Binding investigation between M2-1protein from hRSV and acetylated quercetin derivatives: ^{1}H NMR, fluorescence spectroscopy, and molecular docking

Giovana C. Guimarães [a,b], Hemily R.M. Piva [a,b], Gabriela C. Araújo [b,c], Caroline S. Lima [d], Luis O. Regasini [d], Fernando A. de Melo [b,c], Marcelo A. Fossey [b,c], Ícaro P. Caruso [b,c,*], Fátima P. Souza [b,c,*]

[a] Instituto de Biociências, Letras e Ciências Exatas, UNESP, Department of Biology, São José do Rio Preto, SP, Brazil
[b] Instituto de Biociências, Letras e Ciências Exatas, UNESP, Multiuser Center for Biomolecular Innovation, Laboratory of Molecular Biology, São José do Rio Preto, SP, Brazil
[c] Instituto de Biociências, Letras e Ciências Exatas, UNESP, Department of Physics, São José do Rio Preto, SP, Brazil
[d] Instituto de Biociências, Letras e Ciências Exatas, UNESP, Department of Chemistry and Environmental Sciences, São José do Rio Preto, SP, Brazil

ARTICLE INFO

Article history:
Received 15 November 2017
Received in revised form 21 December 2017
Accepted 24 December 2017
Available online 29 December 2017

Keywords:
M2-1
hRSV
Acetylated quercetin derivatives
^{1}H RMN
Fluorescence spectroscopy
Molecular docking

ABSTRACT

The human Respiratory Syncytial Virus (hRSV) is the main responsible for occurrences of respiratory diseases as pneumonia and bronchiolitis in children and elderly. M2-1 protein from hRSV is an important antitermination factor for transcription process that prevents the premature dissociation of the polymerase complex, making it a potential target for developing of inhibitors of the viral replication. The present study reports the interaction of the M2-1 tetramer with pera (Q1) and tetracetylated (Q2) quercetin derivatives, which were synthesized with the objective of generating stronger bioactive compounds against oxidation process. Fluorescence experiments showed binding constants of the M2-1/compounds complexes on order of 10^4 M^{-1} with one ligand per monomeric unit, being the affinity of Q2 stronger than Q1. The thermodynamic analysis revealed values of $\Delta H > 0$ and $\Delta S > 0$, suggesting that hydrophobic interactions play a key role in the formation of the complexes. Molecular docking calculations indicated that binding sites for the compounds are in contact interfaces between globular and zinc finger domains of the monomers and that hydrogen bonds and stacking interactions are important contributions for stabilization of the complexes. Thus, the interaction of the acetylated quercetin derivatives in the RNA-binding sites of M2-1 makes these potential candidates for viral replication inhibitors.

1. Introduction

The human Respiratory Syncytial Virus (hRSV) is the main cause of respiratory infections as pneumonia and bronchiolitis in children, elderly, and immunocompromised people all over the world [1]. This virus is formed by a nucleocapsid of helical symmetry and lipid envelope with its genome composed of a non-segmented, single-stranded negative sense RNA that having ten coding genes of which encode eleven proteins. Of these proteins, two are expressed by M2 gene which contains two overlapping open reading frames, encoding M2-1 and M2-2 proteins [2].

The hRSV M2-1 protein functions as a transcriptional cofactor of the viral RNA dependent RNA polymerase (RdRp) complex by increasing polymerase processivity and preventing stopping of chain elongation and release of the nascent RNA. Therefore, this RNA-binding protein is an antitermination factor essential for the viral replication that promotes an efficient synthesis of full-length mRNAs of the virus [3,4]. The M2-1 monomer has 194 residues of amino acids that are mainly arranged in α-helices. The tertiary structure is divided into four distinct functionally regions: the thirty-two initial residues in the N-terminal region linked to a zinc finger domain; an α-helix region responsible for the oligomerization; a globular domain capable of binding to the phosphoprotein and RNA; and an unstructured C-terminal region with low degree of conservation. The quaternary structure of the M2-1 is biologically stable at a tetrameric arrangement [5–7].

It is known that previous infections by hRSV do not secure permanent immunity [8]. The usual treatment is not efficient to reduce the hospitalization period of children infected with RSV [9,10]. Many therapies have been developed during the years, as Synagis (palivizumab) an antibody that binds to the fusion protein [11]; the antiviral ribavirin (commercial name Virazole) an analog to the guanosine [12]; and BMS-433771, VP-14637, TMC-353121 compounds that interact with the Tyr198 residue of the F protein and inhibit the viral fusion. However, current treatments against hRSV have shown limitations, including:

* Corresponding authors at: Instituto de Biociências, Letras e Ciências Exatas, UNESP, Multiuser Center for Biomolecular Innovation, Laboratory of Molecular Biology, São José do Rio Preto, SP, Brazil.
E-mail addresses: icarocaruso@sjrp.unesp.br (Í.P. Caruso), fatima@sjrp.unesp.br (F.P. Souza).

https://doi.org/10.1016/j.ijbiomac.2017.12.141
0141-8130/

high cost, substantial side effects, long-term therapy and low efficacy against the virus [11–14].

Quercetin is a natural product belongs a flavonoid class (upside, Fig. 1) and presented potent antiviral activity, exhibiting against several viruses, including hepatitis B virus [15], dengue virus [16], human cytomegalovirus [17], poliovirus type 1 [18], parainfluenza virus type 3 [19], adenovirus [20], and RSV [21]. In a previous paper, we showed the binding of the antitermination factor M2-1 with the quercetin [22]; however, due to the potential oxidation of its hydroxyl groups bound to the aromatic rings, pera (Q1) and tetracetylated (Q2) derivatives (bottom, Fig. 1) were synthetized with objective of generating stronger bioactive compounds which are prone to larger bioavailability. Thus, in the present work we investigated of interaction of the M2-1 protein with acetylated quercetin derivatives (Q1 and Q2) by using fluorescence spectroscopy experiments and molecular docking simulations. The identification and characterization of the compounds Q1 and Q2 were performed by ^{1}H NMR spectroscopy.

2. Materials and methods

2.1. Synthesis, purification and identification of acetylated quercetin derivatives (Q1 and Q2)

Acetylation of quercetin was performed as previously described by Sardi and co-authors, with minor modifications [23]. Quercetin (3.0 g) was dissolved in acetic anhydride (100 mL) and pyridine (100 mL). The mixture was heated at 80 °C for 5 days. After conversion of quercetin confirmed by Thin-Layer Chromatography (TLC) analysis, the reaction medium was poured onto crushed ice. The precipitate was filtered, washed with cold water (3 times) and dried at room temperature. The crude product (2.5 g) was subjected to TLC analysis, using hexane and ethyl acetate (1:1). Revelation of TLC plates under UV light (254 nm) indicated two intense spots, with Retention factor values (Rf) of 0.27 and 0.57.

The crude product (1.8 g) was subjected to chromatography column over silica gel (3 cm × 13 cm) eluted with mixtures of hexane and ethyl acetate, ranging from 20% to 100% of ethyl acetate, yielding 40 fractions (35 mL) (F1–F40). These fractions were combined according to their chromatographic profile delineated by TLC plates developed with hexane and ethyl acetate (1:1). Fractions F4–F10 (Rf = 0.57) and F30–F40 (Rf = 0.27) furnished compounds Q1 (50 mg) and Q2 (20 mg), respectively.

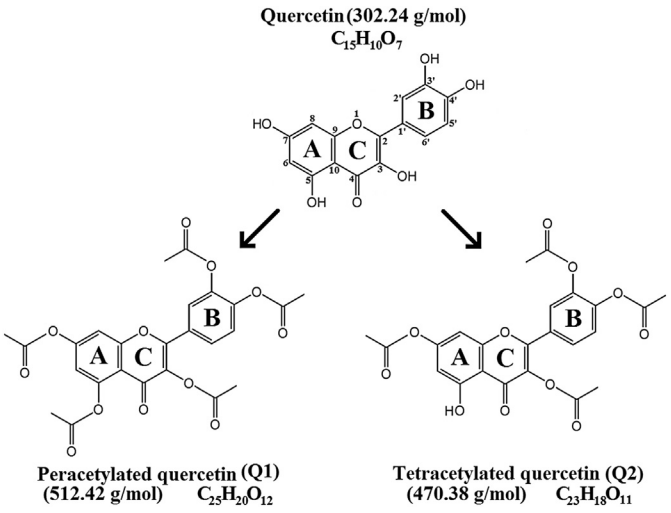

Fig. 1. Molecular structure of the quercetin and its acetylated derivatives Q1 (pera) and Q2 (tetra).

The structure of the compounds Q1 and Q2 was identified by ^{1}H NMR spectra analyses (Supplementary material, Figs. S1–S6). NMR experiments were performed in a Bruker AVANCE III HD (Bruker, Germany) operating at 400 MHz for ^{1}H. The samples of Q1 and Q2 (15 mg) were dissolved in 0.7 mL of deuterated dimethylsulfoxide (DMSO-d_6) and deuterated chloroform ($CDCl_3$), respectively. Chemical shifts (ppm) confirmed acetylation of phenolic quercetin sites, due singlets between 2.33 and 2.35 and 2.36–2.40 ppm for compounds Q1 and Q2, respectively. These signals were attributed to methyl hydrogens of acetyl group (Supplementary material, Figs. S3 and S6).

Peracetylated quercetin (Q1): White solid. ^{1}H NMR (DMSO-d_6, 400 MHz) δ [multiplicity, coupling constant (J)]: 7.19 (d, J = 2.0 Hz, H-6); 7.66 (d, J = 2.0 Hz, H-8); 7.85 (d, J = 2.0 Hz, H-2′); 7.54 (d, J = 8.0 Hz, H-5′); 7,86 (dd, J = 2.0 and 8.0 Hz, H-6′); 2.33–2.34 (s, $\underline{CH_3}CO_2$).

Tetracetylated quercetin (Q2): White solid. ^{1}H NMR ($CDCl_3$, 400 MHz) δ [multiplicity, coupling constant (J)]: 6.62 (d, J = 2.0 Hz, H-6); 6.87 (d, J = 2.0 Hz, H-8); 7.78 (d, J = 2.0 Hz, H-2′); 7.38 (d, J = 8.0 Hz, H-5′); 7,87 (dd, J = 2.0 and 8.0 Hz, H-6′); 12.12 (s, 5-OH); 2.32–2.36 (s, $\underline{CH_3}CO_2$).

2.2. Expression and purification of the M2-1 protein

A M2-1 cDNA from hRSV A2 strain was inserted into pet28A (GE healthcare) vector, allowing the expression of the full-length M2-1 with N-terminal fused to a His_6-tag. M2-1 was expressed and purified as described previously [22], considering that glutathione-affinity chromatography was replaced by Nickel-affinity chromatography, being the protein elution performed by an imidazole gradient.

2.3. Sample preparation for fluorescence experiments

The stock solutions of Q1 (512.42 Da) and Q2 (470.38 Da) were prepared in DMSO at concentrations of 2.6 and 1.1 mM, respectively. The M2-1 sample (3.5 μM/monomer) was prepared in phosphate buffer of 50 mM (pH 7.0) containing 100 mM NaCl. The protein concentration was determined spectrophotometrically (UV–Visible Spectrophotometer, BioMATE 3S, Thermo Scientific, USA) at 280 nm using the molar extinction coefficient of 13,200 $M^{-1}\cdot cm^{-1}$ per monomeric unit [24].

2.4. Fluorescence spectroscopy

The fluorescence quenching experiments were performed using the Cary Eclipse Fluorescence Spectrometer (Varian, USA) with single cell Peltier temperature control and quartz cell of 1.0 cm of optical path length. The emission spectra of the M2-1 in the absence and presence of Q1 and Q2 were collected in the 300–450 nm range with the excitation at 280 nm with the increment of 1.0 nm, ınmwhich was corrected for the background fluorescence of the buffer and for inner filter effects [25]. Both excitation and emission bandwidths were set at 5.0 nmnm. Each point in the emission spectrum is the average of 10 accumulationsınm. The titrations were performed by adding small aliquots from acetylated quercetin derivatives stock solutions to protein solution (2.0 mL) with constant concentration of 3.5 μM at 19, 28, and 37 °C. The compounds concentration varied from 0 to 18.7 μM for Q1 and from 0 to 16.9 μM for Q2. In the analysis of the fluorescence data is admitted that the formation of the protein-ligand complex quenches the emission of the M2–1 after each addition of the compounds and the reminiscent fluorescence corresponds to the unbound protein. Thus, it is possible to calculate the fraction of protein bound (f_B) to the compounds from the fluorescence change with increment of ligand:

$$f_B = \frac{F_0 - F}{F} = \frac{[PL]}{[P_T]} \quad (1)$$

where F_0 and F is fluorescence intensity of the protein in the absence and presence of the compounds, respectively. [PL] is the concentration

of protein bound to n ligands and $[P_T]$is the concentration of total protein. From the fraction of bound protein (f_B) may be determined the fraction of bound ligand (ν) and concentration of free ligand ($[L_F]$) by the following equation:

$$\nu = \frac{[L_b]}{[P_T]} = n \cdot f_B \tag{2}$$

$$[L_F] = [L_T] + n \cdot f_B \cdot [P_T] \tag{3}$$

where n is the number of bound ligands by protein. From the values of ν and $[L_F]$, it is possible to obtain the Scatchard plot ($\nu/[L_F]$ versus ν) for the interaction between M2-1 and compounds (Q1 and Q2). The Scatchard plot was analyzed by using the following equation:

$$\frac{\nu}{[L_F]} = n \cdot K_b - K_b \cdot \nu \tag{4}$$

where K_b is the binding constant for the M2-1/compounds complex, and it is obtained from the slope of the linear fitting. The number of bound ligands (n) is determined from the ordinate and it is used recursively during the fitting process in the Eqs. (2) and (3), until a constant value is achieved at a convergence point and thus the process stops.

2.5. Thermodynamic analysis

The driving forces responsible for the interaction between the M2-1 and the acetylated quercetin derivatives were calculated from the van't Hoff equation:

$$\frac{d}{d\frac{1}{T}} \ln(K_b) = -\frac{\Delta H}{R} \tag{5}$$

where ΔH is the enthalpy changes, R is the universal gas constant and K_b is the apparent dissociation constant at the correspondent temperature (T). The ΔH value was obtained from the slope of the van't Hoff plot, with the respective values of Gibbs free energy changes (ΔG) and entropy change (ΔS) as calculated from the relation:

$$\Delta G = -RT \ln(K_b) \tag{6}$$

$$\Delta S = \frac{\Delta H - \Delta G}{T} \tag{7}$$

2.6. Molecular docking simulation

The crystal structure of the hRSV M2-1 tetramer (PDB ID: 4C3D) [5] was obtained from the Protein Data Bank. Swiss-Model server [26] was used to build some loop regions absent in the crystal structure. The three-dimensional structures of Q1 and Q2 were obtained from Gaussian 09 program [27] using the semi empirical PM6 method for the optimization calculations. AutoDockTools (ADT) [28] was used to prepare M2-1 and acetylated quercetin derivatives by merging non-polar hydrogen atoms, adding partial charges and atom types. The ligand rigid root was generated automatically, setting all possible rotatable bonds and torsions were defining them as active for the compounds. Grid maps were generated with 0.375 Å spacing and dimensions of 126 × 126 × 126 points by the AutoGrid 4.2 program [29], these maps were centered on one of the monomers because of the rotational symmetry of the tetramer (Supplementary material, Fig. S7). The AutoDock 4.2 program was employed to study the binding site between acetylated quercetin derivatives and M2-1 by applying the Lamarckian Genetic Algorithm (LGA) for minimization using a number of energy evaluations of 25 million, a population size of 250 and root-square-mean deviation (RMSD) tolerance for cluster analysis of 2.0 Å. Random starting positions on the entire protein surface and random orientations were used for the ligands. For each docking simulation, 100 different conformers were generated. The representation structural was prepared using PyMOL [30] and the map of interaction was calculated using PoseView [31].

3. Results and discussions

3.1. Characterization of the M2-1/compounds interaction by fluorescence spectroscopy

The titration of the acetylated quercetin derivatives with the M2-1 tetramer caused a decrease in the intensity of the fluorescence signal of the protein (Fig. 1), indicating that the microenvironment of the fluorophores (Tyr and Trp residues) is affected by the presence of Q1 and Q2. Fig. 2 shows the Scatchard plots for the M2-1/compounds interaction generated from fluorescence quenching data (at 340 nm) at 19, 28, and 37 °C. The results of the linear adjustment using the Scatchard equation are presented in Table 1. The binding constants (K_b) determined for the M2-1/compounds complexes are on order of 10^4 M^{-1}, the interaction affinity was found to increase as the temperature increased. Q2 showed a relativity larger affinity than Q1 and also more significant temperature-dependence of its binding constant (Table 1). K_b values for the binding of the acetylated quercetin derivatives to M2-1 are lower than previously reported values for the M2-1/quercetin interaction [22]. The values of number of bound ligands by protein (n) obtained from fitting (Table 1) suggest two possibility for the structural model of interaction: 1) one ligand binds to each monomer of the tetramer; or 2) the binding of the acetylated quercetin derivatives takes place in the interface between the monomers of the tetramer.

The binding constants obtained at varying temperatures were used to evaluate the thermodynamic properties of compounds binding. K_b values were plotted using the van't Hoff equation (Eq. (5)) at 19, 28, and 37 °C (insert in Fig. 2). The plot is linear over the temperature range studied and the enthalpy changes (ΔH) determined from the slope were 1.34 and 2.36 kcal·mol^{-1} for Q1 and Q2, respectively, therefore showing endothermic binding reactions enthalpically unfavorable. The values of ΔG and ΔS were obtained from Eqs. (6) and (7), respectively. $\Delta G < 0$ and $T \cdot \Delta S > 0$ values indicate that the interaction process is spontaneous and entropically favorable. The favorable entropic term provides the major contribution to the Gibbs free energy change, showing that the reaction is entropically driven. The values of $\Delta H > 0$ and $T \cdot \Delta S > 0$ suggest that hydrophobic interactions play a key role in the formation of the M2-1/compounds complexes, as it was determined for the M2-1/quercetin interaction (weak site) [22]. This large positive value of ΔS may be interpreted as a release of ordered water molecules (desolvation) from the binding regions of the compounds in the protein [32]. However, it is not possible to account for the stability of association complexes on the basis of hydrophobic interactions alone, thus the electrostatic contributions should be considered [33].

3.2. Structural model of the M2-1/compounds complexes determined by molecular docking

The fluorescent quenching results were used to drive the molecular docking calculations positioning the compounds Q1 and Q2 as mentioned in Material and Methods (Section 2.6). After 100 runs, the docking output was clustered using RMSD of 2.0 Å and the potential binding site was found taking into account the lowest energy conformer of the compound (Q1 and Q2) from the largest cluster, which is the most populated. Fig. 3A shows the most representative structural model for the interaction of the acetylated quercetin derivatives with the M2-1 protein. The binding region of the compounds in M2-1 takes place in the contact interface between the α-helix 6 of the globular domain (which interacts with phosphoprotein and RNA) of the current chain and the zinc finger domain of the neighbor chain, preceding the structure of the tetramer (Fig. 3B and C). Similar result was determined

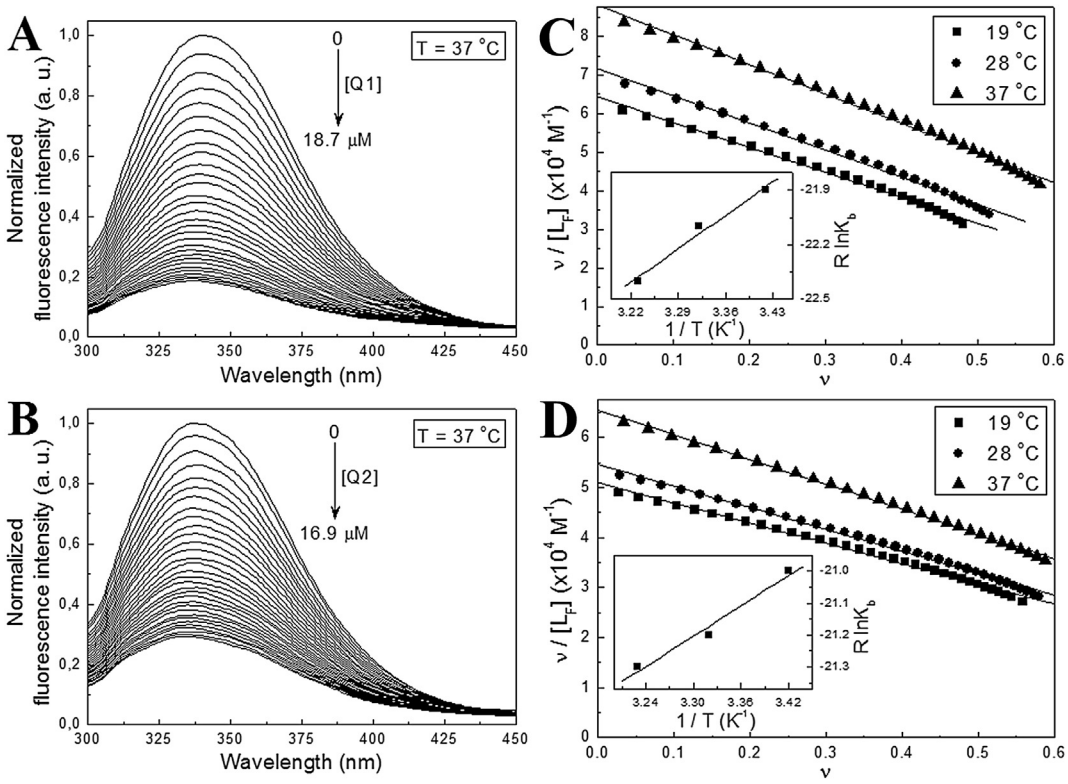

Fig. 2. Emission spectra of M2-1 protein in absence and presence of increments of Q1 (A) and Q2 (B) concentrations (pH 7.0, $T = 37$ °C, $\lambda_{ex} = 280$ nm). [M2-1] = 3.6 μM; [Q1] = 0–18.7 μM, and [Q2] = 0–16.9 μM. Scatchard plot of the interaction between the M2-1 protein and the compounds Q1 (A) and Q2 (B) at three different temperatures (19, 28, and 37 °C). The solid lines denote the linear fitting to the experimental data by using the Scatchard equation (Eq. (4)). The inserts correspond to the van't Hoff plots for the M2-1/compounds complexes. The solid lines depict the linear adjustments to the experimental results by using the van't Hoff equation (Eq. (5)).

computationally for the M2-1/quercetin interaction [22]. Therefore, the results of molecular modeling suggest that the structural model of interaction follows the second possibility raised from the fluorescence data.

Fig. 3D and E show the analysis of the non-covalent interactions in the binding site for Q1 and Q2, respectively. In both sites, hydrophobic contacts, hydrogen bonds, and stacking interactions were determined. For Q1, Lys8D and His22D form hydrogen bonds with the oxygen atoms of the acetyl groups of Q1; Ile173A and Phe23D participate in hydrophobic contacts; and the side chain of Phe23D performs a stacking interaction with the aromatic ring B (Fig. 1). For Q2, Pro6D, Lys8D, and Lys196A make up hydrogen bonds with the acetyl and ketone groups of the compound Q2, being that Lys8D form two; Lys8D, Phe23D, and Ile173A are involved in hydrophobic contacts; and benzene ring of the side chain of Phe23D participates in a stacking interaction with the conjugated rings A and C of Q2. The larger affinity determined experimentally for binding of Q2 than Q1 to M2-1 may be explained by formation of two more hydrogen bonds in the stabilization of the M2-1/Q2 complex.

The analysis of the non-covalent interactions in the binding site (Fig. 3D and E) of the acetylated quercetin derivatives in M2-1 protein shows that Lys8D, Phe23D, and Ile173A are important residues for the binding of these polyphenolic compounds. The balance between hydrophobic contacts (Phe23D and Ile173A), hydrogen bonds (Lys8D), and stacking interaction (Phe23D) determined by the molecular modeling calculations corroborates with the experimental results of the thermodynamic analysis, showing the importance of the hydrophobic contribution for the formation of the association complexes between M2-1 and acetylated quercetin derivatives.

4. Conclusions

The results of the present interaction study show that the acetylated quercetin derivatives Q1 and Q2 can bind to the M2-1 protein with affinity constants on order of 10^4 M^{-1}. The thermodynamic analysis indicates that hydrophobic interaction plays a role key in the formation of the association complexes between M2-1 and compounds. The molecular docking simulations suggest that the possible binding site occurs between the globular domain (especially α-helix 6) from one monomer with the zinc finger domain from the other monomer of the tetramer, and that the hydrogen bonds and stacking interactions promote the

Table 1
Binding constant (K_b), number of bound ligands (n), enthalpy change (ΔH), Gibbs free energy change (ΔG), and entropy change (ΔS) of the M2-1/compounds interaction determined using fluorescence quenching experiments at 19, 28, and 37 °C.

Compounds	T(°C)	K_b ($\times 10^4$ M^{-1})	n	ΔH (kcal · mol^{-1})	ΔG (kcal · mol^{-1})	$T \cdot \Delta S$ (kcal · mol^{-1})
Q1	19	4.03	1.05	1.34	−6.13	7.74
	28	4.37	0.98		−6.37	7.71
	37	4.61	1.00		−6.59	7.93
Q2	19	6.52	1.00	2.36	−6.41	8.77
	28	7.22	1.00		−6.67	9.03
	37	8.27	1.07		−6.95	9.31

All correlations coefficients are ≥0.99.

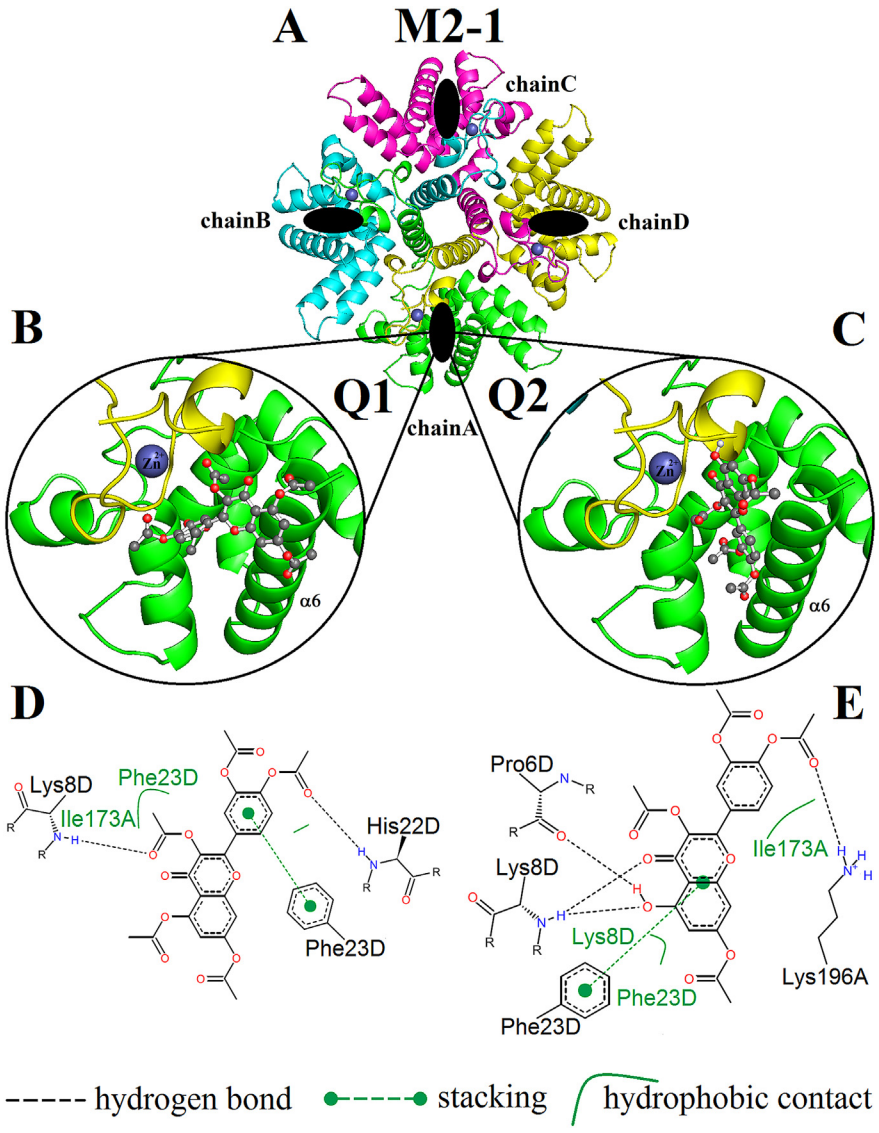

Fig. 3. (A) Location of the compounds Q1 and Q2 in the interface between the monomers of the tetramer of M2-1. The protein is shown as cartoon and the zinc atoms as gray spheres. Three-dimensional structural detail of the microenvironment interaction of Q1 (B) and Q2 (B) in the contact interface between the α-helix 6 (α6) of the globular domain of the current chain (green, chain A) and the zinc finger domain of the neighbor chain (yellow, chain D), preceding the structure of the tetramer. The compounds are shown as stick and ball model (C, gray; O, red). Two-dimensional representation of the non-covalent interactions maps of Q1 (D) and Q2 (E) with the M2-1 protein. The structural representation was performed using PyMOL [30] and the maps of the interactions were calculated using PoseView [31].

stabilization of the M2-1/compounds complexes. Q2 forms two more hydrogen bonds than Q1 in the interaction with M2-1; this fact may explain the higher K_b values of the M2-1/Q2 complex. These findings indicate that acetylated quercetin derivatives could be to test as potential inhibitors of the replication process of hRSV because their probable binding sites take place in the RNA-binding region, corresponding to the globular and zinc finger domain. This fact may have an important implication for developing a new strategy of treatment against the viral infection.

Acknowledgments

This work was supported by Fundação de Amparo à Pesquisado Estado de São Paulo (FAPESP 2013/24355-2 and 2009/53989-4). We thank Prof. Dr. Altair Benedito Moreira for the access to the fluorescence spectrometer (FAPESP 2014/17511-0), Prof. Dr. Alexandre Suma de Araújo for the access to the Calix cluster for performing the molecular docking simulations (FAPESP 2010/18169-3), Prof. Dr. Marcio Francisco Colombo for the access to the Äkta purifier, and GridUNESP for the availability of Gaussian 09 quantum chemical program.

Appendix A. Supplementary data

Supplementary data to this article can be found online at https://doi.org/10.1016/j.ijbiomac.2017.12.141.

References

[1] H. Grosfeld, M.G. Hill, P.L. Collins, RNA replication by respiratory syncytial virus (RSV) is directed by the N, P, and L proteins; transcription also occurs under these conditions but requires RSV superinfection for efficient synthesis of full-length mRNA, J. Virol. 69 (1995) 5677–5686.
[2] P.L. Collins, Y.T. Huang, G.W. Wertz, Identification of a tenth mRNA of respiratory syncytial virus and assignment of polypeptides to the 10 viral genes, J. Virol. 49 (1984) 572–578.
[3] R. Fearns, P.L. Collins, Role of the M2-1 transcription antitermination protein of respiratory syncytial virus in sequential transcription, J. Virol. 73 (1999) 5852–5864.

[4] P.L. Collins, M.G. Hill, J. Cristina, H. Grosfeld, Transcription elongation factor of respiratory syncytial virus, a nonsegmented negative-strand RNA virus, Proc. Natl. Acad. Sci. U. S. A. 93 (1996) 81–85.
[5] S.J. Tanner, A. Ariza, C.A. Richard, H.F. Kyle, R.L. Dods, M.L. Blondot, W. Wu, J. Trincão, C.H. Trinh, J.A. Hiscox, M.W. Carroll, N.J. Silman, J.F. Eléouët, T.A. Edwards, J.N. Barr, Crystal structure of the essential transcription antiterminator M2-1 protein of human respiratory syncytial virus and implications of its phosphorylation, Proc. Natl. Acad. Sci. U. S. A. 111 (2014) 1580–1585.
[6] R.W. Hardy, G.W. Wertz, The Cys3-His1 motif of the respiratory syncytial virus M2-1 protein is essential for protein function, J. Virol. 74 (2000) 5880–5885.
[7] T.-L. Tran, N. Castagné, V. Duboscland, S. Noinville, E. Koch, M. Moudjou, C. Henry, J. Bernard, R.P. Yeo, J.-F. Eléouët, The respiratory syncytial virus M2-1 protein forms tetramers and interacts with RNA and P in a competitive manner, J. Virol. 83 (2009) 6363–6374.
[8] E.E. Walsh, D.R. Peterson, A.R. Falsey, Risk factors for severe respiratory syncytial virus infection in elderly persons, J. Infect. Dis. 189 (2004) 233–238.
[9] H.M. Corneli, J.J. Zorc, P. Majahan, K.N. Shaw, R. Holubkov, S.D. Reeves, R.M. Ruddy, B. Malik, K.A. Nelson, J.S. Bregstein, K.M. Brown, M.N. Denenberg, K.A. Lillis, L.B. Cimpello, J.W. Tsung, D.A. Borgialli, M.N. Baskin, G. Teshome, M.A. Goldstein, D. Monroe, J.M. Dean, N. Kuppermann, Bronchiolitis Study Group of the Pediatric Emergency Care Applied Research Network (PECARN), A multicenter, randomized, controlled trial of dexamethasone for bronchiolitis, N. Engl. J. Med. 357 (2007) 331–339.
[10] C.P. Guideline, Diagnosis and management of bronchiolitis, Pediatrics 118 (2006) 1774–1793.
[11] J.M. Geskey, N.J. Thomas, G.L. Brummel, Palivizumab: a review of its use in the protection of high risk infants against respiratory syncytial virus (RSV), Biologics 1 (2007) 33–43.
[12] R.W. Sidwell, D.L. Barnard, Respiratory syncytial virus infections: recent prospects for control, Antivir. Res. 71 (2006) 379–390.
[13] K. Kimura, S. Mori, K. Tomita, K. Ohno, Antiviral activity of NMSO3 against respiratory syncytial virus infection in vitro and in vivo, Antivir. Res. 47 (2000) 41–51.
[14] C. Cianci, N. Meanwell, M. Krystal, Antiviral activity and molecular mechanism of an orally active respiratory syncytial virus fusion inhibitor, J. Antimicrob. Chemother. 55 (2005) 289–292.
[15] K. Zandi, B.T. Teoh, S.S. Sam, P.F. Wong, M.R. Mustafa, S. Abubakar, Antiviral activity of four types of bioflavonoid against dengue virus type-2, Virol. J. 8 (2011) 560–571.
[16] G.Y. Zuo, Z.Q. Li, L.R. Chen, X.J. Xu, In vitro anti-HCV activities of *Saxifraga melanocentra* and its related polyphenolic compounds, Antivir. Chem. Chemother. 16 (2005) 393–398.
[17] D.L. Evers, C.F. Chao, X. Wang, Z. Zhang, S.M. Huong, E.S. Huang, Human cytomegalovirus-inhibitory flavonoids: studies on antiviral activity and mechanism of action, Antivir. Res. 68 (2005) 124–134.
[18] H.J. Choi, J.H. Kim, C.H. Lee, Y.J. Ahn, J.H. Song, S.H. Baek, D.H. Kwon, Antiviral activity of quercetin 7-rhamnoside against porcine epidemic diarrhea virus, Antivir. Res. 81 (2009) 77–81.
[19] G. Xu, J. Dou, L. Zhang, Q. Guo, C. Zhou, Inhibitory effects of baicalein on the influenza virus in vivo is determined by baicalin in the serum, Biol. Pharm. Bull. 33 (2010) 238–243.
[20] J. Johari, A. Kianmehr, M.R. Mustafa, S. Abubakar, K. Zandi, Antiviral activity of baicalein and quercetin against the Japanese encephalitis virus, Int. J. Mol. Sci. 3 (2012) 16785–16795.
[21] T.N. Kaul, E. Jr Middleton, P.L. Ogra, Antiviral effect of flavonoids on human viruses, J. Med. Virol. 15 (1985) 71–79.
[22] T.S.P. Teixeira, I.P. Caruso, B.R.P. Lopes, L.O. Regasini, K.A. Toledo, M.A. Fossey, F.P. Souza, Biophysical characterization of the interaction between M2-1 protein of hRSV and quercetin, Int. J. Biol. Macromol. 95 (2017) 63–71.
[23] J.D.C.O. Sardi, C.R. Polaquini, I.A. Freires, L.C. de Carvalho Galvão, J.G. Lazarini, G.S. Torrezan, P.L. Rosalen, Antibacterial activity of diacetylcurcumin against *Staphylococcus aureus* results in decreased biofilm and cellular adhesion, J. Med. Microbiol. 66 (2017) 816–824.
[24] E. Gasteiger, C. Hoogland, A. Gattiker, S. Duvaud, M.R. Wilkins, R.D. Appel, A. Bairoch, Protein identification and analysis tools on the ExPASy server, in: John M. Walker (Ed.), The Proteomics Protocols Handbook, Humana Press 2005, pp. 571–607.
[25] J.R. Lakowicz, Principles of Fluorescence Spectroscopy, second ed. Kluwer Academic Publishers/Plenum Press, New York, 1999.
[26] M. Biasini, S. Bienert, A. Waterhouse, K. Arnold, G. Studer, T. Schimidt, F. Kiefer, T.G. Cassarino, M. Bertoni, L. Bordoli, T. Schwede, SWISS-MODEL: modelling protein tertiary and quaternary structure using evolutionary information, Nucleic Acids Res. 42 (2014) 252–258.
[27] M.J. Frisch, G.W. Trucks, H.B. Schlegel, G.E. Scuseria, M.A. Robb, J.R. Cheeseman, G. Scalmani, V. Barone, B. Mennucci, G.A. Petersson, H. Nakatsuji, M. Caricato, X. Li, H.P. Hratchian, A.F. Izmaylov, J. Bloino, G. Zheng, J.L. Sonnenberg, M. Hada, M. Ehara, K. Toyota, R. Fukuda, J. Hasegawa, M. Ishida, T. Nakajima, Y. Honda, O. Kitao, H. Nakai, T. Vreven, J.A. Montgomery Jr., J.E. Peralta, F. Ogliaro, M. Bearpark, J.J. Heyd, E. Brothers, K.N. Kudin, V.N. Staroverov, R. Kobayashi, J. Normand, K. Raghavachari, A. Rendell, J.C. Burant, S.S. Iyengar, J. Tomasi, M. Cossi, N. Rega, J.M. Millam, M. Klene, J.E. Knox, J.B. Cross, V. Bakken, C. Adamo, J. Jaramillo, R. Gomperts, R.E. Stratmann, O. Yazyev, A.J. Austin, R. Cammi, C. Pomelli, J.W. Ochterski, R.L. Martin, K. Morokuma, V.G. Zakrzewski, G.A. Voth, P. Salvador, J.J. Dannenberg, S. Dapprich, A.D. Daniels, O. Farkas, J.B. Foresman, J.V. Ortiz, J. Cioslowski, D.J. Fox, Gaussian 09, Revision A.02, Gaussian, Inc., Wallingford CT, 2009.
[28] M.F. Sanner, Python: a programming language for software integration and development, J. Mol. Graph. Mod. 17 (1999) 57–61.
[29] G.M. Morris, D.S. Goodsell, R.S. Halliday, R. Huey, W.E. Hart, R.K. Belew, A.J. Olson, Automated docking using a Larmarckian genetic algorithm and an empirical binding free energy function, J. Comput. Chem. 19 (1998) 1639–1662.
[30] W.L. Delano, The PyMOL Molecular Graphics System, DeLano Scientific, San Carlos, CA, USA, 2002.
[31] P. Fricker, M. Gastreich, M. Rarey, Automated generation of structural molecular formulas under constraints, J. Chem. Inf. Comput. Sci. 44 (2004) 1065–1078.
[32] A. Hatsumi, Y. Magobei, Thermodynamic characterization of drug binding to human serum albumin by isothermal titration microcalorimetry, J. Pharm. Sci. 83 (1994) 1712–1716.
[33] P.D. Ross, S. Subramanian, Thermodynamics of protein association reactions: forces contributing to stability, Biochemistry 20 (1981) 3096–3102.